Adjustable Chirp Injection-Locked 1.55-μm VCSELs for Enhanced Chromatic Dispersion Compensation at 10-Gbit/s

Bo Zhang[1], Xiaoxue Zhao[2], Louis Christen[1], Devang Parekh[2], Werner Hofmann[3], Ming C. Wu[2], Markus C. Amann[3], Connie J. Chang-Hasnain[2] and Alan E. Willner[1]

[1]*Department of Electrical Engineering - Systems, University of Southern California, Los Angeles, CA 90089, Email: boz@usc.edu*

[2]*Department of Electrical Engineering and Computer Sciences, University of California, Berkeley, CA 94720*

[3]*Walter Schottky Institute, Technical University of Munich, Am Coulombwall 3, 85748 Garching, Germany*

Abstract: We demonstrate adjustable negative chirp from a directly-modulated, injection-locked 1.55-μm VCSEL by controlling the injection parameters. Chromatic dispersion tolerance is enhanced by greater than 10X at 10-Gb/s compared to that of a free-running VCSELs.

OCIS codes: (230.2035) Dispersion compensation devices, (250.7260) Vertical cavity surface emitting lasers

1. Introduction

Vertical-cavity surface-emitting lasers (VCSELs) are highly desirable for cost-effective wavelength-division-multiplexed (WDM) optical communication systems because of their excellent single-mode behavior and potential for low-cost manufacturing and electronic integration [1]. However, to become a promising transmitter for metro-area applications, VCSELs have to exhibit properties such as broad modulation bandwidth and negligible frequency chirp.

Optically-injection-locked (OIL) VCSELs, which are locked, both in frequency and phase, to a master laser by photon injection at similar wavelength, have been demonstrated to be effective for enhancing the small-signal modulation bandwidth [2], as well as reducing the frequency chirp of directly modulated diode lasers [3]. Hence, (OIL) VCSELs can be a promising candidate for future metro-area networks.

Frequency chirp reduction using optical injection locking has been shown both theoretically and experimentally [4]. However, little has been studied on time-resolved chirp waveforms and the chirp polarity, which are closely correlated to the link dispersion. Furthermore, it would be extremely valuable to be able to tune the chirp such that its magnitude can be dynamically reconfigured according to the link for flexible dispersion compensation.

In this paper, we demonstrate experimentally that the frequency chirp of OIL VCSELs is not only reduced in magnitude but also switched in sign, for the first time. We show that the change of the chirp polarity from positive to negative is due to an interesting phenomenon of data inversion in OIL VCSELs. Furthermore, by adjusting the injection power ratio, the negative peak-to-peak chirp can be effectively controlled. Measured time-resolved chirp waveforms verify this chirp tunability. Chromatic dispersion compensation is investigated at 10-Gb/s, and more than 125-km standard single-mode fiber (SSMF) only transmission with negligible power penalty at a bit-error-rate (BER) of 10^{-9} is achieved using OIL VCSELs. This shows a factor of 10 larger dispersion tolerance compared to that of a free-running directly-modulated VCSEL.

2. Concept and experimental setup

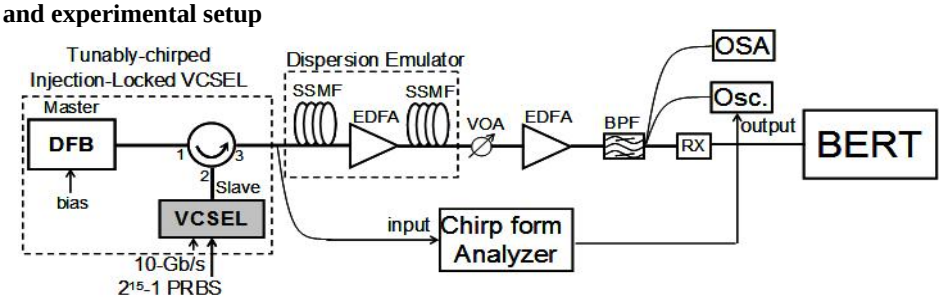

Fig. 1 Experimental setup. OIL VCSELs with tunable chirp for dispersion compensation. Chirp form analyzer is used to investigate the polarity flipping of the frequency chirp. Multiple spools of SSMF are used to study the effect of the flipped chirp on chromatic dispersion.

The experimental setup is shown in Fig. 1. A distributed feedback (DFB) laser serves as the master laser to injection-lock a 1.55-μm VCSEL. An optical circulator is placed in between the DFB and the VCSEL to achieve unidirectional locking. The VCSEL current is directly modulated at 10-Gb/s, with a 2^{15}-1 pseudorandom binary sequence (PRBS). Both the VCSEL bias and the data driving voltage are optimized. The DFB current is adjusted to control the power injecting into the VCSEL. Chromatic dispersion is emulated using variable lengths of SSMF

spools with EDFAs in between. The fiber link is estimated to be linear with < 3.5-dB power into the SSMF. A pre-amplified receiver and an error detector are used for BER quantification of the signal quality with and without fiber transmission. The Advantest Q7606B chirp-form analyzer is used together with a sampling oscilloscope to obtain the time-resolved chirp waveforms and the intensity waveforms at various injection ratio levels.

3. Tunable chirp and dispersion compensation enhancement

The time-resolved intensity and chirp waveforms for a free-running VCSEL directly modulated at 10-Gb/s are shown in Fig. 2 (a), with light and dark lines respectively. The device is biased at 5.5 mA and the driving voltage is 1-Vpp. The adiabatic chirp depends strongly on the optical intensity and appears as a frequency shift according to the ON/OFF signal. The transient chirp appears at the rising and falling edges of the signal as spikes. This is defined as the "positive chirp" due to the positive frequency deviation on the rising edge and negative frequency deviation on the falling edge. Positive chirp speeds up pulse broadening when transmitting through standard positive dispersion fiber, thus increases power penalty [5]. It is obvious that for the free-running case, the adiabatic chirp dominates and the peak-to-peak chirp is > 25 GHz. Fig. 2 (b-d) shows the intensity and chirp waveform when the VCSEL is injection-locked at various injection ratios. Chirp reduction is evident compared to the free-running case while the transient chirp now becomes the dominant part. By adjusting the power of the DFB laser and the coupling to the VCSEL, one can control the injection ratio, which is defined as the power ratio of the injected light to the VCSEL emission. When the injection ratio is increased from 6.21 dB to 8.58 dB and to 11.12 dB, the peak-to-peak chirp is reduced from 3.1 GHz to 2.7 GHz and then to 1.55 GHz, respectively, as shown in Fig. 2 (b, c, d). This can be understood from the fact that strong injection reduces the carrier density change and thus the index variation during the same transition time, as compared to weak injection.

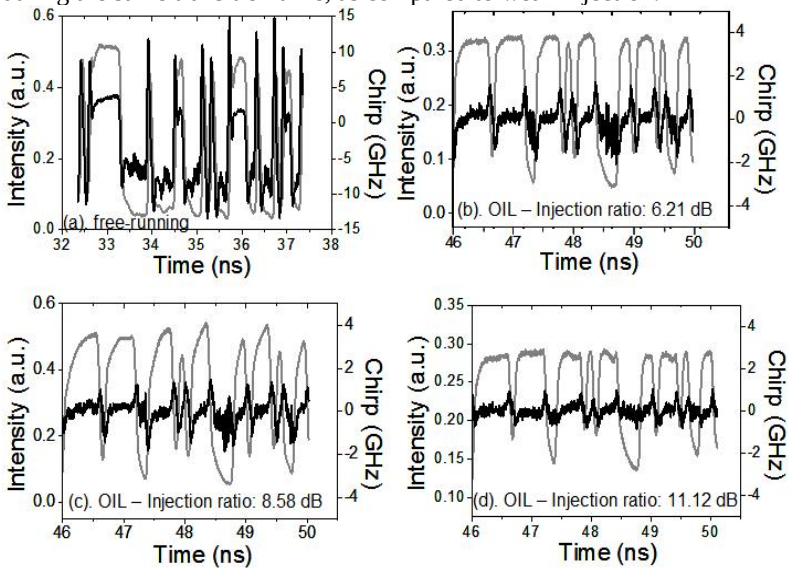

Fig. 2

Fig. 3

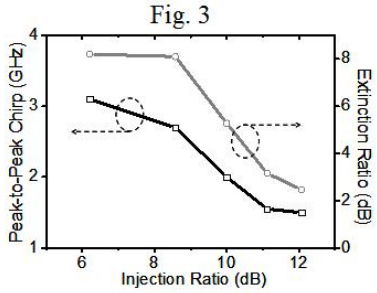

Fig. 4

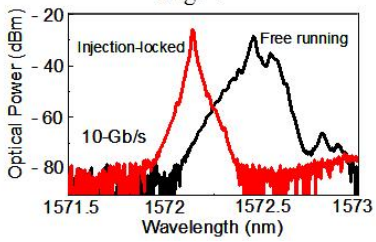

Fig. 2. Experimental measurement of time-resolved chirp and intensity waveforms at 10-Gb/s for (a) free-running VCSEL, (b-d) OIL VCSEL with injection ratios of (b) 6.21 dB (c) 8.58 dB (d) 11.12 dB. Fig. 3. Peak-to-peak chirp and extinction ratio at 10-Gb/s as functions of injection ratio. Fig. 4. Optical spectra of free-running and OIL VCSEL with 8.58-dB injection ratio, both modulated at 10 Gbit/s.

Fig. 3 quantifies the peak-to-peak chirp tunability as a function of the injection ratio. The chirp can be reduced to half of its original value by increasing the injection ratio from 6.21 dB to 12.07 dB. However, a tradeoff exists between the chirp and the extinction ratio of the signal. The degradation of the extinction ratio is inevitable at strong injection conditions due to the surface normal geometry of the VCSEL. Therefore, the injection ratio needs to be optimized. Fig. 4 shows the optical spectra of both free-running and OIL VCSEL with an 8.58-dB injection ratio under 10-Gb/s large signal modulation. The much broader and asymmetric free-running spectrum indicates the dominant adiabatic chirp and the unbalanced transient chirp. With injection locking, the spectrum is greatly narrowed because of the chirp reduction. The locked wavelength is also blue-shifted to the master wavelength.

One remarkable difference between the chirp waveforms of a free-running and an injection-locked VCSEL shown in Fig. 2 is the polarity flipping of the transient chirp from "positive" to "negative", which manifests itself as negative frequency deviation on the rising edge and positive deviation on the falling edge. This presents a significant advantage for transmission over SSMF due to the narrowing rather than the broadening of the pulse in its initial stage of propagation. We found that the reason for the negative chirp from directly-modulated OIL VCSEL is data

pattern inversion. This phenomenon is repeatedly observed on different devices when the coupling lensed-fiber is spatially adjusted. The VCSELs used in the experiment have an aperture size of 5 μm [6]. The pattern inversion occurs when the lensed-fiber is slightly off the center of the laser aperture, where the fundamental transverse mode emission is the strongest. We attribute this phenomenon to modal competition, as discussed in [7], where optical data inversion was achieved by injecting a modulated master laser to lock onto a higher order transverse mode of a slave VCSEL. However, in our case, the VCSEL is directly modulated by a large signal and the locking is on the fundamental mode. The modulation is thus transferred to the injection ratio (P_{master} / P_{slave}) with an inverted pattern, because bit "1" gives a large P_{slave}. With the 5-μm aperture, the VCSEL waveguide actually supports higher order transverse modes, although it emits a single fundamental mode under free-running condition due to a larger match of the gain and the modal profile. However, if the lensed-fiber is moderately tuned away from the center of the aperture, the external light injection will possibly excite a higher order transverse mode of the device. A higher order transverse mode usually possesses a wavelength 5-nm shorter than that of the fundamental mode. The wavelength of the external injection light, however, is usually close to the fundamental mode with the aim of locking the lasing mode of a free-running laser. When the current applied to the VCSEL is a bit "0", the injection ratio is high, the fundamental mode is locked due to the wavelength alignment, despite the spatial preference of the higher order mode. Therefore, the output is relatively high in intensity (output bit "1"). Whereas if the current applied to the VCSEL is a bit "1", the injection ratio is low, the spatial coupling may be more effective such that it excites some of the higher order transverse modes. Thus, the fundamental mode output power, which is still the locked output, is reduced, leading to a bit "0". This results in the inversion of the data pattern. Detailed theoretical study is under way.

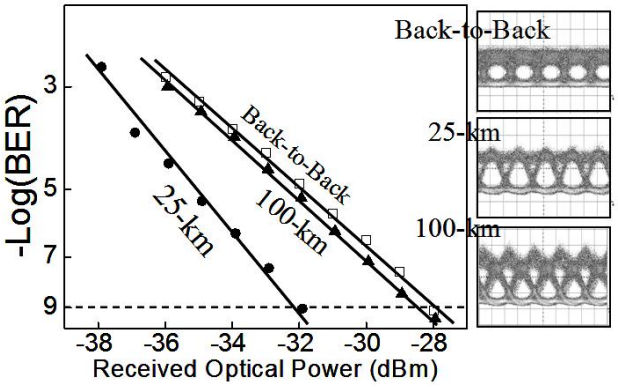

Fig. 5. BER measurements and error-free eye diagrams of an OIL VCSEL with back-to-back, 25-km and 100-km SSMF transmission.

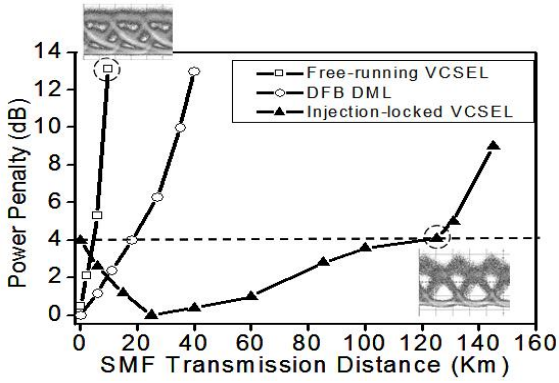

Fig. 6. Power penalty vs. SSMF transmission distance for free-running VCSEL, commercial DFB DML and OIL VCSEL.

In order to demonstrate the benefit of the tunable negative chirp, we perform chromatic dispersion tolerance comparison between free-running and OIL VCSELs by transmitting 10-Gb/s signals through SSMF with variable lengths. Fig. 5 shows the BER measurements of an OIL VCSEL at 10-Gb/s. After 25-km SSMF, the power penalty reduction reaches its maximum and a 4-dB penalty improvement is achieved at a BER of 10^{-9}. Even 100-km SSMF transmission shows no penalty for a BER of 10^{-9}. These results can be explained by the fact that negative frequency chirping interacts beneficially inside the SSMF. The pulse initially narrows as it propagates inside the fiber and reaches a minimum width at a certain distance (25-km in this case). After that, the pulse starts to broaden due to the onwards dispersion. The three inset eye diagrams in Fig. 5 clearly show pulse narrowing after 25-km transmission and broadening after 100 km. Fig. 6 quantifies the power penalty with increased SSMF distance. Due to the large positive adiabatic chirp, the 10-Gb/s free-running VCSEL can transmit no more than 5 km with more than 4-dB power penalty. Even for a 10-Gb/s commercial DFB directly-modulated laser (DML) with standard positive chirp, the transmission distance is still limited to be less than 20 km for a 4-dB power penalty. For OIL VCSELs, even though there is some back-to-back penalty (due to extinction ratio degradation), the signal is actually regenerated because of the negative chirp, and there is no observed penalty after 125-km of uncompensated SSMF transmission. This performance is more than 10X better than that of a free-running VCSEL or a DFB DML [8].

4. References

[1] C. Chang-Hasnain, et. *al*., *IEEE Journal of Quantum Electron.*, vol. 27, no. 6, pp. 1402-1409, (1991)
[2] L. Chrostowski, X. Zhao, and C. J. Chang-Hasnain, *IEEE Trans. Microw. Theory Tech.* 54, 788-796 (2006)
[3] S. Mohrdiek, et. *al*., *IEEE Journal of Lightwave Technol.*, vol. 12, no. 3, pp. 418–424, (1994)
[4] C. Chang, et. *al*., *IEEE Journal of Lightwave Technol.*, vol. 9, no. 5, pp. 1386, (2003)
[5] A. H. Gnauck, et. *al*., *IEEE Photon. Technol. Lett.*, vol. 3, pp. 916, (1991)
[6] M. Ortsiefer, et. *al*., *Electron. Lett.* vol. 39, no. 24, pp. 1731-1732, (2003)
[7] Y. Onishi, et. *al*., *IEEE Journal of Selected Topics in Quantum Electron.*, vol. 11, pp. 999-1005, (2005)
[8] L.-S. Yan, et. *al*., *Optics Express.* vol. 13, pp. 5106-5115 (2005)